International Journal of Bioelectromagnetism
IJBEM

Volume 3, Number 2, pp. 20-30, 2001.

Impedance Cardiography

Pasi K. Kauppinen[(a)], Jari Hyttinen[(a)], Tiit Kööbi[(b)], Seppo Kaukinen[(c)], Jaakko Malmivuo[(a)]

[(a)]Ragnar Granit Institute, Tampere University of Technology, Tampere, Finland
[(b)]Department of Clinical Physiology, Tampere University Hospital, Tampere, Finland
[(c)]Department of Anesthesia and Intensive Care, Tampere University Hospital, Tampere, Finland

Correspondence: PK Kauppinen, Ragnar Granit Institute, Tampere University of Technology,
P.O. Box 692, FIN-33101 Tampere, Finland.
E-mail: pasi.kauppinen@tut.fi, phone +358 3 247 4012, fax +358 3 247 4013

Abstract. Impedance cardiography (ICG) estimates cardiac function from a single waveform measured at body surface, that reflects an integrated combination of complex sources. ICG is a simple method, which has nevertheless failed to achieve wide clinical acceptance. Measured data remain controversial, leading sometimes to errors and discouraging utilization of the approach. Models underlying the development of ICG have been inaccurate. The purpose of this present work was to develop ICG measurement configurations with application of lead field theory and computer modeling. The measurement properties of ICG were studied showing that the method is not specifically sensitive to detect conductivity changes in the regions assumed to be the source of ICG. Means were devised to develop alternative, more sensitive ICG configurations based on the 12-lead electrocardiography (ECG) electrode system. As compared with conventional ICG, more selective measurements were obtained. Several configurations were preliminarily tested on healthy volunteers and patients undergoing valve replacement. Valvular disease was distinguished within the study population and recorded 12-lead ICG signals evinced waveforms and landmarks different from those of conventional ICG. Computerized volume conductor modeling proved to be a powerful method in analyzing and developing ICG. The results suggest that ICG producing more direct physiological data can be obtained.

1. Introduction

An ideal method of assessing information on the cardiovascular system should be noninvasive, simple, atraumatic, inexpensive, reliable and also applicable in long-term surveillance outside the cardiac monitoring laboratory. Conventional impedance cardiography (ICG) techniques provide a single impedance tracing, from which parameters related to the pump function of the heart such as cardiac output (CO) are estimated. Most of the properties of ICG render it superior to other methods, the prominent exception being its limited reliability, which has hampered its acceptance as a clinical method. When the notion of impedance is transferred to the biological tissues in the human body and to applications seeking to quantify physiological function from measured data, the investigator moves into an area complex and incompletely understood.

1.1. Conventional ICG

Measurement of thoracic electrical impedance has been practiced since the 1930s [Nyboer, 1970]. The first practical method for determination of cardiac function in a clinical setting was introduced by Kubicek et al. in the 1960s, together with the original CO formula based

on elementary physics [Kubicek, 1989; Kubicek et al., 1966; Patterson et al., 1964]. Several variations in electrode configurations and CO equations have been presented over the years to improve the method [Bernstein, 1986; Penney et al., 1985; Woltjer et al., 1995].

Basic Principle

The impedance (Z) is a function of the cross-sectional area (A) and length (l) between the voltage pick-up electrodes applied on the volume conductor. In terms of segmental *volume* (v), (Z) or alternatively resistance R is given by

$$R = \rho \frac{l}{A} = \rho \frac{l^2}{v} \qquad (1)$$

where l is the voltage pick-up electrode separation.

Nyboer [Mohapatra, 1981; Nyboer, 1970] assumed that the pulsatile flow of blood could be modeled as the resistance of the blood pulse, R_b, in parallel with the steady basal value of resistance, R_0, of the surrounding tissue, forming a total resistance R_n

The resistance change ΔR due to the addition of blood volume Δv is derived from Eq. 1 as follows:

$$\Delta R = R_n - R_0 = \rho l^2 \left(\frac{v_1 - v_0}{v_0 v_1} \right) = - \frac{\rho l^2 \Delta v}{v_0 v_1} \approx - \frac{\rho l^2}{v^2} \Delta v \qquad (2)$$

where v_0 is the original volume of the object and v_1 the volume after the addition of blood, which for small changes in v is $v_0 \approx v_1$. Substituting Eq. 1 and rearranging, Nyboer's formula is obtained

$$\Delta R = -R^2 \frac{\Delta v}{\rho l^2} \quad \Leftrightarrow \quad \Delta v = -\Delta R \frac{\rho l^2}{R^2} \qquad (3)$$

This equation describes the relationship between the volume of a blood pulse and the related resistance change. The model constitutes an oversimplified view of any physiological system.

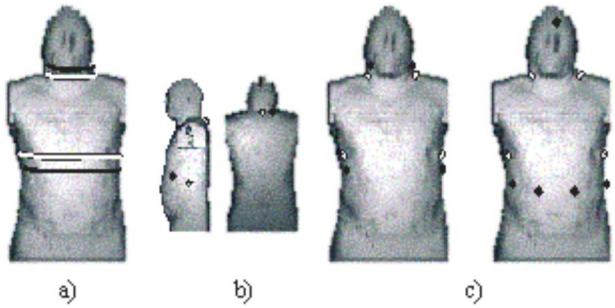

Figure 1. Various electrode configurations for ICG reported in the literature. a) the conventional band, b) four-spot, c) eight-spot and d) nine-spot electrode configurations. Locations of black spots are used for current injection and white spots for voltage detection in actual measurements.

Various ICG Methods

Since the functioning of the heart is obviously the generator of measurable cyclic impedance variation, many investigators have sought to evolve methods for CO derived from this periodic signal applying various modifications to the Eqs. 1 – 3 or electrode configurations.

Fig. 1 shows several configurations reported in the literature. The well-established band electrode method by Kubicek has been replaced by various spot electrode configurations in the effort to improve patient comfort and the practicality of the method without significantly changing the signal content.

1.2. Field Theoretical Analyses of ICG

Although much work has been done to date, the development of ICG is still principally based on the same ideology introduced decades ago, relying strongly on an empirical approach. Use of over-simplified models has limited and confined improvement in the technique because of the gap between the model and the anatomy and physiology of the system investigated.

Computer models designed to calculate the current flow in the thorax have been used more recently in examining the ICG measurement configurations, producing supporting data for the anticipated conception of the complexity of the signal origin [Kim et al.,1988; Wang and Patterson, 1995; Wtorek and Polinski, 1995].

A theoretical foundation exists for analysis of the measurement sensitivity distribution of ICG based on the lead field theory introduced in the 1950s for bio-electric (i.e. ECG) analysis and later in the 1970s [Geselowitz, 1971] for bio-impedance (BI) measurements. BI measurement sensitivity distribution reflects how conductivity changes throughout the volume affect the measured data. The application of lead field theory in ICG has not evolved to its potential; only initial studies with analytical models have hitherto been conducted to estimate the measurement sensitivity distribution in cylindrically shaped objects with uniform conductivity [Penney et al., 1979].

1.3. Objectives of this Study

The purpose here was to utilize the lead field theoretical approach in investigating the information content of existing ICG measurement configurations, and in examining possibilities of recording ICG within the clinical setting of the 12-lead ECG based on computerized application of the lead field theory in realistically shaped volume conductors.

2. Material and Methods

2.1. ICG Sensitivity Distribution

The sensitivity distribution of a BI measurement gives a relation between the impedance (and change in it) caused by a given conductivity distribution (and its change). It describes how effectively each region is contributing to the measured *Z*. If conductivity change is not involved, the measured impedance *Z* is obtained with

$$Z = \int_{v} \frac{1}{\sigma} \bar{J}_{LE} \cdot \bar{J}_{LI} \, dv \qquad (4)$$

where $\bar{J}_{LE}$ and $\bar{J}_{LI}$, obtained with reciprocal energization, are the current density fields (*i.e.* impedance measurement lead fields) associated with the current injection and voltage measurement leads [Kauppinen, 1999; Malmivuo and Plonsey, 1995]. This equation gives the contributions from each region to the total impedance, and the dot product of the two fields expresses the sensitivity of the measurement to conductivity changes throughout the volume conductor.

The impact of a certain conductivity variation in different regions depends on the sensitivity field. As the scalar field may possess positive and negative values depending on the orientation of the two lead fields, the measured impedance may either increase, decrease or be entirely unaffected in consequence of a conductivity change in a particular region.

The relative magnitude of the sensitivity field in a tissue type (or a group of tissues

considered as one target volume) gives a measure of how conductivity variation in that tissue will affect the detected DZ. The overall sensitivity of a tissue type is obtained by integrating the sensitivity values of the tissue over the volume it occupies. This sensitivity value can then be compared with the absolute total sensitivity of the model as given by

$$\frac{\sum_{i=1}^{n_g} A_i \Delta V_i}{\sum_{\substack{\text{all tissues} \\ \text{or groups}}} \left| \sum_{i=1}^{n_t} A_i \Delta V_i \right|} * 100\% \qquad (5)$$

where n_g is the number of elements in the target volume and n_t the number of tissue elements of a certain type. The denominator is the sum of the absolute partial contributions from all tissues (or tissue groups), and the numerator is the contribution of the target tissue.

2.2. Volume Condutor Computer Models

Utilizing Eq. 4 with finite difference method (FDM) computer modeling, information as to the respective capacity of different ICG measurements to detect conductivity and its changes in the thorax can be estimated. Methods to construct and solve accurate volume conductor computer models based on the FDM have been previously developed and validated [Kauppinen et al., 1999].

Three different anatomy models were employed in the study:

Visible Human Man model.

A particularly accurate source of anatomical data, the U.S. National Library of Medicine's Visible Human Man (VHM) [Ackerman et al., 1991; Spitzer et al., 1996] was employed as basis for detailed FDM modeling. The original cryosection images are 2048 by 1216 pixels in 24-bit color, resulting in about 14 gigabytes of data in size. A total of 118 cryosection images from the top of the head to the pelvis were segmented using a volume segmentation method which directly provides volume elements of anatomy data for FDM mesh generation [Heinonen et al., 1998]. For data storage and image analysis the accuracy of the images was reduced to 250x250 pixels using an 8-bit gray scale colormap. The resolution was from 0.044 to 5.7 cm^3.

Dynamic Model - Diastolic & Systolic models.

The ECG triggered end-systolic and end-diastolic MR image data sets used by Wang and Patterson [Wang and Patterson, 1995] were segmented. A two-phase thorax model (i.e. two models of the same person at different moments of the cardiac cycle) was constructed from these data producing end diastole model (EDM) and end systole model (ESM). The number of voxels was equal in both models, as the segmented outermost layer from the first data set was used as base for segmentation of the other set. Both models consisted of 70 slices and 30 tissue types. The resolution of FDM elements in the ECG-triggered models varied from 0.10 to 5.8 cm^3 resulting to 121431 elements.

2.3. Analysis of Conventional ICG Electrode Configutations

Contributions to the sensitivity distribution were assessed with the VHM thorax model for four ICG electrode configurations utilizing conventional band electrodes or modifications replacing the bands with spot electrodes (see Fig. 1):

a) Original configuration by Kubicek et al. using four band electrodes [Kubicek et al., 1966]

b) Configuration by Penney et al. using four spot electrodes [Penney et al., 1985]

c) Configuration by Bernstein using eight spot electrodes [Bernstein, 1986]

d) Configuration proposed by Woltjer et al. using nine spot electrodes [Woltjer et al., 1996].

Simulations were conducted to obtain the basal impedance, Z_0, lead fields in the thorax generated by the current and the measurement leads $\bar{J}_{LE}$ and $\bar{J}_{LI}$, and the resulting measurement sensitivity distribution according to the Eqs. 4 and 5.

2.4. Derivation and Analysis of 12-lead ICG Measurement Configurations

The prospects of recording multiple ICG waveforms with more selective sensitivity to particular regions of the thorax were investigated employing the 12-lead electrode system. The lead field concept can be applied, facilitating synthesis of leads with desired properties, e.g., more specific leads.

The nine electrode locations of the 12-lead ECG electrode system were used separately to calculate a basic set of lead fields for each model, the VHM and two-phase models. A computer algorithm was developed to make combinations with the 12-lead electrode system using at maximum four electrodes at a time for either lead field in Eq. 4. Deriving ICG measurement combinations with the pre-calculated lead fields is a non-iterative calculation, since the system is assumed to be linear. E.g. a lead field between the chest leads V1 and V6 may be obtained by subtracting $V1_{LL}$ from $V6_{LL}$. A total of 65476 impedance measurement configurations utilizing the 12-lead electrode locations was thus derived.

A database was computed for each model and measurement configuration containing the information on the formation of Z_0 and proportional contributions according to Eq. 5. This was done for each classified tissue and for a number of different tissue groups reflecting functional structures of the cardiovascular system. Further, the same calculations were applied to the data produced by subtracting the sensitivity and Z_0 values simulated by the ECG-triggered models EDM and ESM.

2.5. Experimental Clinical Measurements

An experimental pilot study was conducted to evaluate the impedance waveforms detected by the 12-Lead configurations selected based on the simulations. The study involved 12 healthy volunteers and a group of 9 patients with valvular heart disease (3 mitral, 6 aortic).

The measurements were performed by CircMonä B202 (JR medical Ltd, Tallinn, Estonia), which includes an impedance channel delivering 0.7 mA at 30 kHz in combination with a devised front-end apparatus [Kauppinen et al., 1999], that enables to record multiple 12-lead ICG signals with digitally controlled electrode configurations.

2.6. Analysis and Comparison of Clinical and Simulated Data of 12-Lead ICG

The theoretical data from the models were compared between each model and the data from the test measurements. The clinical data was compared between the two study groups consisting of healthy volunteers and valvular patients.

Triggering to the R-peak of ECG, ensemble averaged measured DZ signals were calculated for each configuration and subject. Several parameters were derived from the data measured from the volunteers: minimum and maximum Z_0, DZ_{max} indicating the maximum impedance deflection of averaged DZ, DZ_{vent} the amplitude of ventilation effect during the recording period of each configuration, ratio of DZ_{max}/DZ_{vent}, and the mean absolute percentage error (MAPE) between the individual average DZ and the average DZ calculated from all the volunteers. MAPE describes the difference between an individual DZ and the average DZ obtained from the study group with particular configuration. The parameters were computed as average values from each subject for each configuration. Correlation matrix was calculated between the derived parameters and the simulated sensitivity distributions. In addition, the inter-group (volunteers versus patients) differences (MAPEs) were calculated

for the averaged DZs.

3. Results

3.1. Simulated Sensitivity Distributions

Conventional ICG electrode configurations

The conventional band electrode configuration and alternative configurations suggested to replace the bands were shown not to be specifically sensitive in measuring conductivity changes in regions generally considered important in measuring SV or CO, namely the heart, lungs or aorta and other large vascular trees. More than half of the measurement sensitivity in each case studied was concentrated in the skeletal muscle, while less than 5 % was in the heart region and the large vessels. Furthermore, the results showed heterogeneous current field flow in the thorax, and modifying the electrode configuration resulted in different sensitivity distributions which must have an influence on the composition of measured signals. This is further illustrated in the frontal and transversal sensitivity images shown in Fig. 2. Sensitivity at the mid-frontal plane was most uniform with the band setting and least uniform with the eight-spot setting. Using the band electrodes the transversal sensitivity image showed a significant source of signal from the posterior side of the thorax. The four-spot configuration caused a more concentrated current flow in the left side of the thorax, which increased the sensitivity on that side.

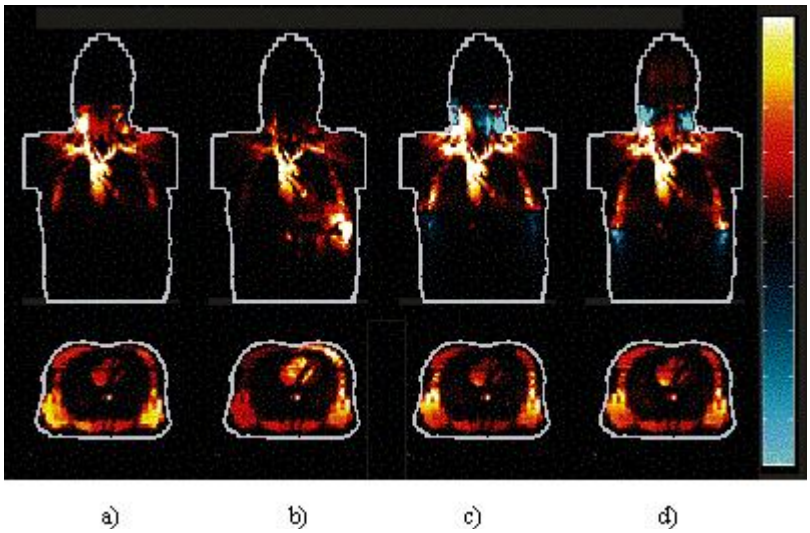

Figure 2. Mid-frontal and transversal views of sensitivity field distributions. a) conventional band, b) four-spot, c) eight-spot and d) nine-spot configurations. Zero sensitivity is indicated with black colour, positive sensitivities are visualized with hot colourmap and negative with cool colourmap.

12-Lead ICG

Simulations revealed that as compared to conventional ICG, clearly enhanced sensitivities can be obtained in various regions of the cardiovascular system by appropriately selecting the measurement configurations used for ICG. Figure 3 summarises the simulated measurement sensitivities of the configurations discussed above. Values are indicated for each tissue type in addition to three tissue groups consisting of pulmonary circulation, systemic circulation and all the blood masses and the heart muscle. For the tissues of the cardiovascular structures, a maximum of 75 % proportional sensitivity was attained. The agreement between the different models was notable and the values in Fig. 3 are averages as calculated from the three models.

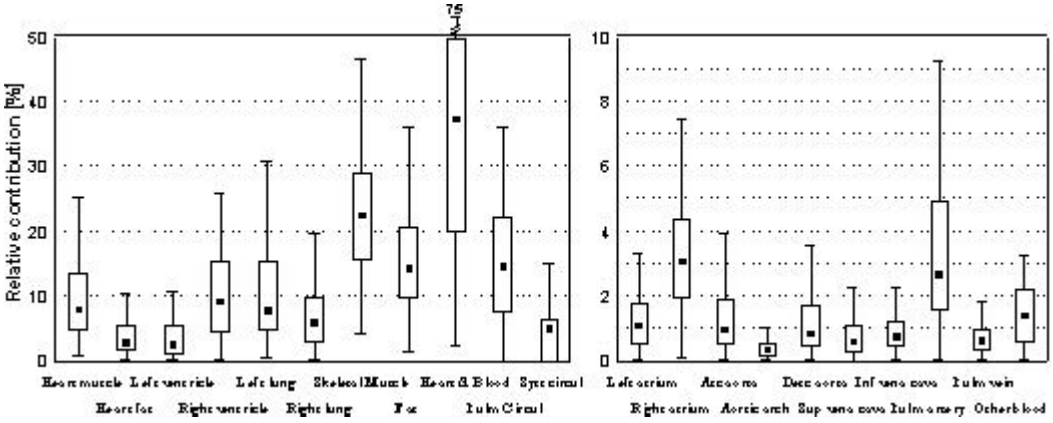

Figure 3. Sensitivities in different tissues for the configurations selected for clinical experiments. Values are calculated as averages from the three different models. The median of the values is represented by the smallest box in the plot, the spread (variability) by the quartiles (the 25th and 75th percentiles) and the minimum and maximum values of the sensitivity among the configurations.

3.2. Correlation Data

For the Z_0 the simulated values showed statistically significant correlation between the models ($p<0.008$).

The calculated correlation matrix showed a large number of statistically significant relationships between the simulated data and the parameters derived from the measurements. The strongest value for correlation was 0.45 as calculated between the positive area after the R-peak and the sensitivity proportion in right ventricle in ESM ($p<0.000$) and also for the MAPE after the R-peak and the Z_0 change between the ECG triggered models ($p<0.000$). DZ_{max} did not show correlation to Z_0 simulated with any of the models, but significant correlation was found to the DZ calculated by subtracting values of Z_0 calculated with the EDM and ESM ($r=0.30$, $p<0.000$). Proportional sensitivity change as calculated with the EDM and ESM correlated positively with DZ_{max} when investigating the heart region ($r=0.31$, $p<0.000$), while negative correlation was found for the sensitivity in the lungs.

3.3. Inter-Individual Variations within Volunteers

Generally, increasing MAPEs correlated positively with the Z_0 difference between the triggered models ($r=0.24…0.44$, $p<0.000$), the sensitivity change in the fat and skeletal muscle ($r=0.24…0.43$, $p<0.000$) and also the heart region $r=0.29…0.37$, $p<0.000$). Negative correlations (i.e. smaller MAPE with higher sensitivity) were evident for lung configurations

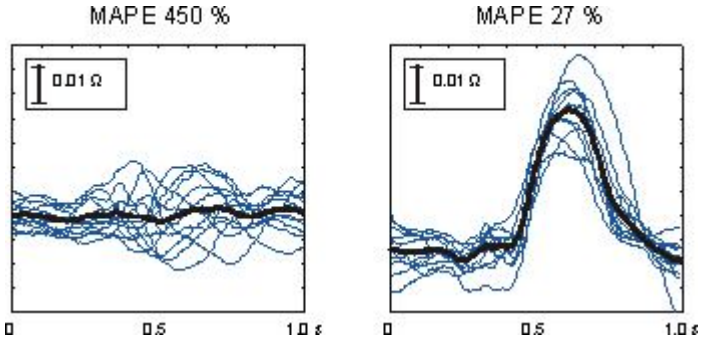

Figure 4. DZ waveforms obtained with two different configurations exhibiting the smallest and largest variations (MAPE) between the volunteers. Thin lines show individual averaged DZ, thicker tracing the average from all the volunteers.

with all of the three models ($r=-0.23…-0.32$, $p<0.000$), but not for the sensitivity change obtained by subtracting the triggered model values, and for the tissue groups consisting of

either pulmonary or systemic circulation. Fig. 4 shows averaged DZs from the volunteers for the configurations producing the smallest (27%) and the largest (450%) inter-individual MAPEs for the period of the whole cardiac cycle.

3.4. Differences Between Volunteers and Patients

The inter-group MAPEs between the volunteers and the valvular patients showed the highest positive correlation to the sensitivity in VHM heart muscle ($r=0.36$, $p<0.000$). MAPE before the R-peak correlated positively to the sensitivity change between the triggered models in the atria ($r=0.38$, $p<0.000$), and after the R-peak to the heart muscle and left ventricle ($r=0.20$, $p<0.003$). The largest negative correlation was found for the sensitivity in the lungs in the triggered models ($r=-0.25$, $p<0.000$). Example averaged DZs recorded from both of the study populations are shown in Fig. 5.

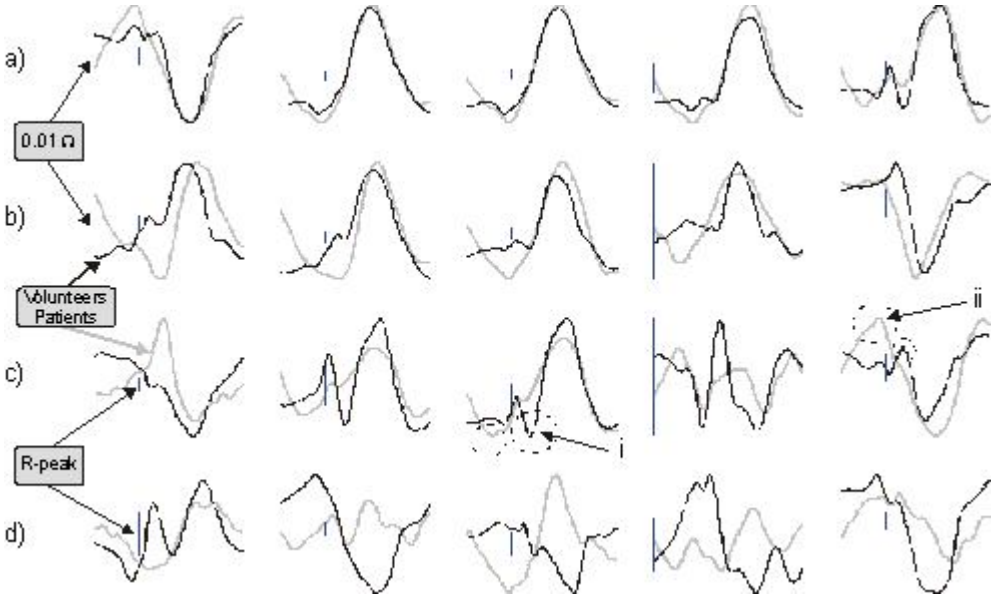

Figure 5. Examples of the 12-lead based ICG recordings shown as average signals from the study groups (volunteers and valvular patients). a) Tracings with small inter-group variation, b) changes between the groups in the time instant of the maximum impedance deflection, c) characteristic signals with notable peaks or deflections missing between the groups, d) large inter-group MAPEs. For explanation of tracings marked i and ii, please refer to text.

Certain configurations recorded similar waveforms between the study groups (a), several produced similar shapes in the impedance deflection but shifting the time instant of the peak change (b). The maximum impedance deflection was more often delayed than advanced with the patients when compared to the healthy subjects although the patients heart rate was higher (average HR: volunteers 62, patients 71). Fig. 5 c) shows configurations with additional or missing deflections between the study groups, and d) data with larger deviations between the groups. Investigating DZs from individuals reveals a tendency shown in the averaged signals, although some configurations seem to detect regional information and thus producing more diversified impedance curves. As an example, in (c) the distinct peak marked i occurs in the data recorded from 11/12 volunteers, but not in any patient. The peak marked ii, on the other hand, is elevated in 6/9 patients and in only one volunteer.

4. Discussion

Computer Models.

The anatomical differences between the VHM and the two-phase models were considerable; for instance, the total volumes were 47 and 21 l for the VHM and the two-phase models, respectively. In spite of this, the most selective configurations for certain anatomical region or tissue were identical independent of the model applied. This result was unexpected, since

to achieve high sensitivity in a certain region and low in others requires in principle a measuring configuration where lead fields of current and voltage electrodes are practically perpendicular to each other. Slight deviations in model geometry or electrode locations could then markedly modify the partial sensitivity values.

Conventional ICGs.

Simulation results emphasized the multiregional sampling sensitivity of the studied ICG configurations. For the conventional ICGs, only an approximately 5 % contribution from all blood masses and cardiac tissue was detected. This can be taken to imply that the valuable information, i.e. the information needed to determine the CO or other desired parameters, overlaps with a wide range of other information unretrievable from DZ. Although useful information has been obtained from the ICG waveform, it originates from a multiplicity of sources with unpredictably varying contributions depending on the characteristics and hemodynamic condition of the subject. Thus, particular caution is called for when applying ICG to clinical work. It is unlikely that a universally ideal electrode configuration providing accurate measurements exists for ICG. If the number of unpredictable factors contributing to or modifying the ICG waveform are many, at least as many specific measurements should be taken as there are contributing factors to establish the state of the system.

12-Lead ICG.

Numerical modeling with the lead field theoretical approach made possible detailed analysis of a large number of configurations. Increasing the contribution from a limited region may improve the physiological relevance of recorded data, which was achieved in theory with the regional multi-electrode measuring configurations. According to simulations, for the tissues of the cardiovascular structures, a maximum of 75 % proportional sensitivity was attained. For the aortas and vena cavas the values were relatively small, since the electrode locations of the 12-lead system are not favorable for vertical measurements. Although highly elevated sensitivities were obtained, it was not possible to achieve fully selective measurements for any of the tissues. Moreover, even with these enhanced measuring configurations, everything still affects everything; nonetheless their relative contributions should be more favorable than in conventional methods to produce regional information.

Clinical Experiments.

Weak, but statistically significant relationships between the simulated data and the parameters derived from the measurements were attained indicating the general ability of the modeling approach in developing and understanding the properties of various electrode configurations applied in ICG. Recorded 12-lead signals had characteristic landmarks not coincing with those of conventional ICG, indicating varied information content between the configurations. Furthermore, signals were noted showing a suggestive resemblance to invasive data and morphological variations in disease not present with conventional ICG. Valvular disease was detected when investigating at least two signals simultaneously; a single ICG signal cannot produce information for the identification of the existence of the disease. An important limitation in the clinical measurements is the instrumentation restricting the analysis of collected signals since only one channel can be recorded at a time.

Future Research.

On the theoretical side, extending the two-phase to a multi-phase model one could simulate the ΔZ waveform and investigate geometrical and conductivity changes separately and not only assess the sensitivity distribution at one time instant. Comparisons with clinical data would facilitate the development of models and provide a guide in selecting valid tissue conductivities. Further research is clearly needed to determine the precise effects of 1) inter-individual variations, 2) postural changes and 3) breathing on a) sensitivity distributions and b) measured data. Future studies should also take account of the effects of slight positional changes of electrodes. To collect a wide range of clinical data also from patients during invasive measurements, the system should be implemented in a multi-channel form allowing parallel recording of all *independent* impedance signals. A multi-channel ICG

instrumentation would be practical in prospective 12-lead measurements reducing the overall recording time and allowing analyses of signals recorded simultaneously. A large diverse group of patients in each disease category should be investigated pre- and postoperatively prior to drawing any definite conclusions about the 12-lead ICG measurements.

5. Conclusions

Estimation of CO from a non-invasively measured impedance signal is an ill-posed inverse problem with no unique solution, since DZ is always a combined presentation of multiple sources. An ICG method could be made more reliable by sampling the target region with several electrode settings giving emphasis to the particular region. The results obtained demonstrate the feasibility of the lead field method in developing ICG. Recorded 12-lead ICG signals exhibited landmarks not coincing with those of conventional ICG showing morphological variations in disease. Configurations producing regional information may have a range of applications apart from the CO estimation. However, understanding the information conveyed by the 12-lead ICG requires multi-phase modelling and measurements with simultaneous acquisition of hemodynamic variables such as flow and pressure in the structures of the cardiovascular system. This calls for more advanced multi-channel instrumentation for testing the methodology in clinical environment.

Acknowledgements

This work was supported financially by the Ragnar Granit Foundation. The authors wish to thank Professor Robert Patterson, University of Minnesota, for supplying the MRIs for the two-phase model.

References

Ackerman MJ. The Visible Human Project. *Journal of Biocommunications,* 18: 14, 1991.

Bernstein DP. A new stroke volume equation for thoracic electrical bioimpedance: theory and rationale. *Critical Care Medicine,* 14: 904-909, 1986.

Geselowitz DB. An application of electrocardiographic lead theory to impedance plethysmography. *IEEE Transactions on Biomedical Engineering,* 18: 38-41, 1971.

Heinonen T, Dastidar P, Kauppinen P, Malmivuo J and Eskola H. Semi-automatic tool for segmentation and volumetric analysis of medical images. *Medical & Biological Engineering & Computing,* 36: 291-296, 1998.

Kauppinen P. Application of lead field theory in the analysis and development of impedance cardiography. PhD Thesis, Tampere University of Technology, Tampere, Finland, 1999.

Kauppinen P, Hyttinen J, Laarne P and Malmivuo J. A software implementation for detailed volume conductor modelling in electrophysiology using finite difference method. *Computer Methods and Programs in Biomedicine,* 58: 191-203, 1999.

Kauppinen PK, Hyttinen JAK, Kööbi T and Malmivuo J. Multiple lead recordings improve accuracy of bio-impedance plethysmographic technique. *Medical Engineering & Physics,* 21: 371-375, 1999.

Kim DW, Baker LE, Pearce JA and Kim WK. Origins of the impedance change in impedance cardiography by a three-dimensional finite element model. *IEEE Transactions on Biomedical Engineering,* 35: 993-1000, 1988.

Kubicek WG. On the source of peak first time derivative (dZ/dt) during impedance cardiography. *Annals of Biomedical Engineering,* 17: 459-462, 1989.

Kubicek WG, Karnegis JN, Patterson RP, Witsoe DA and Mattson RH. Development and evaluation of an impedance cardiac output system. *Aerospace Medicine,* 37: 1208-1212, 1966.

Malmivuo J and Plonsey R. Bioelectromagnetism: Principles and Application of Bioelectric and Biomagnetic Fields. Oxford University Press, New York, 1995.

Mohapatra SN. Non-invasive Cardiovascular Monitoring by Electrical Impedance Technique. Pitman, London, 1981.

Nyboer J. Electrical Impedance Plethysmography. Charles C Thomas, Springfield, 2nd ed,1970.

Patterson RP, Kubicek WG, Kinnen E, Witsoe DA and Noren G. Development of an electrical impedance plethysmography system to monitor cardiac output. In proceedings of the 1st Annual Rocky Mountain Bioengineering Symposium, 1964, 56-71.

Penney BC, Narducci LM, Peura RA, Anderson FAJ and Wheeler HB. The impedance plethysmographic sampling field in the human calf. *IEEE Transactions on Biomedical Engineering,* 26: 193-198, 1979.

Penney BC, Patwardhan NA and Wheeler HB. Simplified electrode array for impedance cardiography. *Medical & Biological Engineering & Computing,* 23: 1-7, 1985.

Spitzer V, Ackerman MJ, Scherzinger AL and Whitlock D. The visible human male: a technical report. *Journal of the American Medical Informatics Association*, 3: 118-130, 1996.

Wang L and Patterson R. Multiple sources of the impedance cardiogram based on 3-D finite difference human thorax models. *IEEE Transactions on Biomedical Engineeringg*, 42: 141-148, 1995.

Woltjer HH, Arntzen BW, Bogaard HJ and de Vries PM. Optimalisation of the spot electrode array in impedance cardiography. *Medical & Biological Engineering & Computing*, 34: 84-87, 1996.

Woltjer HH, van der Meer BJ, Bogaard HJ and de Vries PM. Comparison between spot and band electrodes and between two equations for calculations of stroke volume by means of impedance cardiography. *Medical & Biological Engineering & Computing*, 33: 330-334, 1995.

Wtorek J and Polinski A. Examination of impedance cardiography properties--FEM model studies. *Biomedical Sciences Instrumentation*, 31: 77-82, 1995.